

# Rectangular Gilbert Tessellation

Emily Ewers\* and Tatyana Turova †

## Abstract

A random planar quadrangulation process is introduced as an approximation for certain cellular automata describing neuronal dynamics. This model turns out to be a particular (rectangular) case of a well-known Gilbert tessellation. The central and still open question is the distribution of the line segments. We derive exponential bounds for the tail of this distribution. The correlations in the model are also investigated for some instructive examples. In particular, the exponential decay of correlations is established. If the initial configuration of points is confined in a box  $[0, N]^2$  it is proved that the average number of rays escaping the box has a linear order in  $N$ .

## 1 Introduction

### 1.1 From cellular automata to a planar quadrangulation

The random quadrangulation process of a square in a plane considered here is motivated by a study [4] of cellular automata introduced to describe neuronal activity. Let us briefly recall that in [4], a propagation of electrical impulses (or activation) in a network on a finite set of vertices  $V_N := [0, N]^2 \subset \mathbb{Z}^2$  is designed as follows.

The vertices represent neurons, while the edges of the lattice  $\mathbb{Z}^2$  are associated with synaptic connections. Hence, each vertex  $v$  is connected to its four nearest neighbours which make a set

$$N_v := \left\{ v + \{(0, -1), (0, 1), (-1, 0), (1, 0)\} \right\} \cap V_N.$$

The set of vertices  $V_N$  is split into subsets

$$\begin{aligned} V^- &= \{(x, y) \in V_N : x, y \text{ both even}\}, \quad \text{and} \\ V^+ &= V_N \setminus V^-. \end{aligned}$$

---

\*Mathematics Department, RPTU Kaiserslautern-Landau, Gottlieb-Daimler-Straße 48, 67663 Kaiserslautern, Germany, emily.ewers@rptu.de

†Mathematical Center, University of Lund, Box 118, Lund S-221 00, Sweden, tatyana@maths.lth.se

All vertices in  $V^-$  are assigned *inhibitory* type, while all vertices in  $V^+$  are assigned *excitatory* type.

Let  $X_v(t) \in \{0, 1\}$  denote the state at the vertex  $v$  at time  $t$ :  $X_v(t) = 1$  is *active* state and  $X_v(t) = 0$  is *nonactive*. Given the set of initially active vertices

$$A(0) = \{v \in V : X_v(0) = 1\} =: U \subseteq V,$$

the dynamics of process  $X(t) = (X_v(t), v \in V)$  in discrete time  $t \geq 1$  is defined as follows:

$$X(t+1) = \begin{cases} 1, & \text{if } |N_v \cap V^+ \cap A(t)| - |N_v \cap V^- \cap A(t)| \geq 1, \\ 0, & \text{otherwise.} \end{cases} \quad (1)$$

In words this definition reflects the properties of excitatory neurons to facilitate the propagation of activity, while the inhibitory neurons, on the contrary, prevent propagation of activity. These two actions make the behaviour of the system non-monotone.

It also follows from definition (1) that a neuron, which has more excitatory active neighbours than inhibitory active ones, becomes active, regardless of its own type.

The focus of study of this model is the evolution of the set of active vertices

$$A_U(t) = \{v \in V : X_v(t) = 1\}$$

for any given initial state  $U$ . By the definition (1) we have for all  $t \geq 0$

$$A(t+1) = \{v \in V : |N_v \cap V^+ \cap A(t)| - |N_v \cap V^- \cap A(t)| \geq 1\}.$$

The question of interest concerns the limiting states for such a process. Depending on the initial configuration of active vertices, qualitatively different limiting spatio-temporal states may appear. They are described in [4] as patterns of activity expanding with constant rate, fixed contours of constant activity, or stable patterns moving across the network. Notably, the lattice structure with its symmetries plays an important role here, particularly in formation of the last two classes of the limiting states.

It must be admitted, however, that a rigorous analysis of the model [4] is still beyond reach. Therefore one may consider first some particular cases. It is shown ([4], Section 3.6) that when the initial set  $U$  is sparse (more precisely, if  $(x, y)$  is a vector between arbitrary two points in  $U$ , then  $\min\{|x|, |y|\}$  should be larger than some absolute constant), the evolution of  $(A_U(t), t \geq 0)$  is described straightforward as follows.

**Definition 1.1.** *From each vertex in a given set  $U \subset V_N := [0, N]^2 \subset \mathbb{Z}^2$  a line begins to grow at time  $t = 0$  along the edges of the lattice in both opposite directions, adding one edge per time step; with probability  $\frac{1}{2}$  these directions are set to be either vertical or horizontal. As soon as a line meets another line or the boundary of  $V_N$ , the growth stops.*

Again, due to the discrete structure of a lattice there could be not only collisions of orthogonal lines but also "head-on" collisions of lines. Thus, it is natural to study as an approximation for a model given by Definition 1.1, a similar (and seemingly simpler) process of growing rays but on  $\mathbb{R}^2$  in which we rediscover a well-known model of Gilbert as we see in a moment.

## 1.2 Model of planar quadrangulation

**Definition 1.2.** Let  $\mathcal{V}_N$  be a finite set of points in  $\Lambda_N = [0, N]^2 \subseteq \mathbb{R}^2$ . For each  $u \in \mathcal{V}_N$  a random direction  $d_u$  is assigned independently:

$$\mathbb{P}\{d_u = \text{horizontal}\} = p = 1 - \mathbb{P}\{d_u = \text{vertical}\}.$$

From each point into each side of the assigned direction a ray grows with constant speed 1 until it either intersects another ray or the boundary of the box  $\Lambda_N$ .

By this definition the rays within box  $\Lambda_N$  stop growing after at most time  $N$ . The process is illustrated in Figure 1.

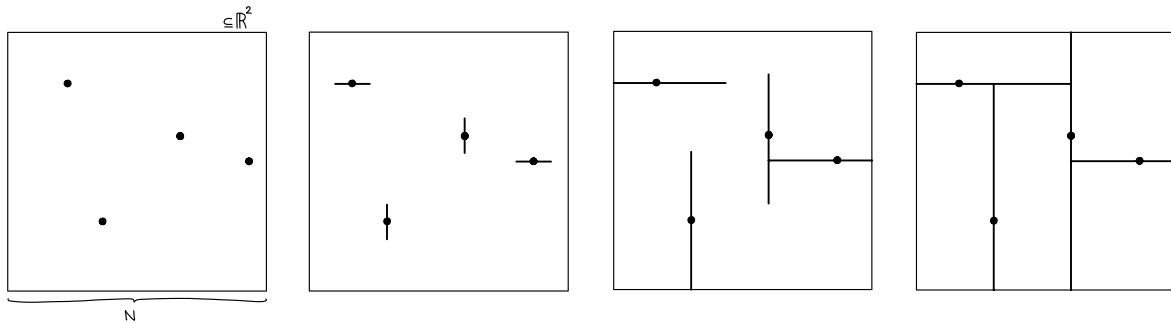


Figure 1: Example of a process with four points from the left to the right: (1) at  $t = 0$ , (2) at some moment before any collision, (3) at the time of the first collision, (4) at  $t = N$ .

We assume that the initial set  $\mathcal{V}_N$  is random

$$\mathcal{V}_N = \Omega \cap \Lambda_N, \tag{2}$$

where  $\Omega$  denotes a Poisson point process in  $\mathbb{R}^2$  with constant intensity  $\lambda > 0$ . Hence, the number of vertices in  $\mathcal{V}_N$  (denoted  $|\mathcal{V}_N|$ ) follows a  $\text{Poi}(\lambda N^2)$ -distribution.

The initial conditions, i.e. set  $\mathcal{V}_N$  and the directions  $d_v, v \in \mathcal{V}_N$ , are the only source of randomness, otherwise, the dynamics are deterministic. When the process stops growing rays within  $\Lambda_N$ , all faces in the resulted configuration are almost surely rectangles, and moreover all the junctions except the corners of the box itself are  $T$ -shaped. An example of such a quadrangulation of a square is shown in Figure 2.

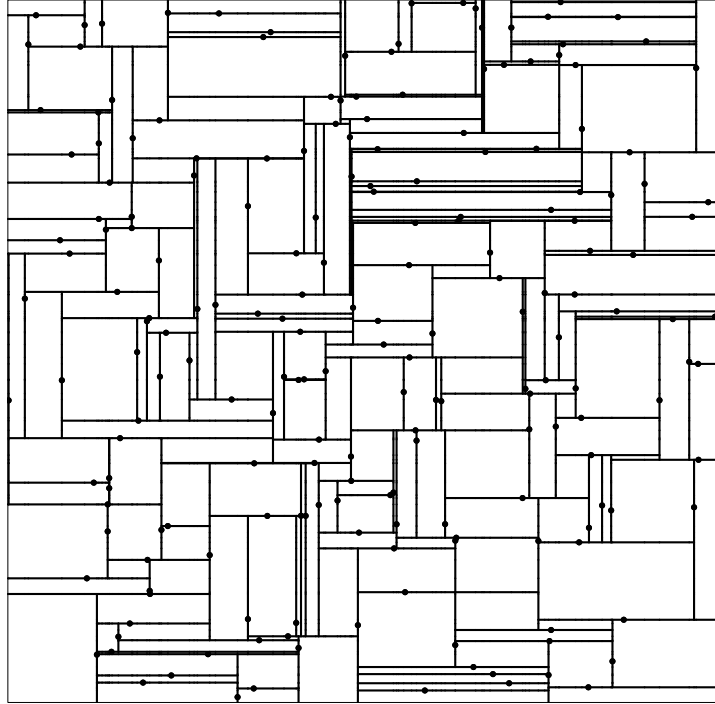


Figure 2: Example of a random quadrangulation that is obtained from the model in  $\mathbb{R}^2$  presented in this work.

### 1.3 Gilbert tessellation

It is remarkable that the model in Definition 1.2 turns out to be a particular case of Gilbert tessellation introduced already in 1967 by E.N. Gilbert [6]. In fact, originally Gilbert defined and studied a much more general model on  $\mathbb{R}^D$  in [5] inspired by the facts on crystals growing in a metal or mineral (if  $D = 3$ ). Furthermore, Gilbert wrote "The "crystals" may also be cells in living tissue" [5], to which statement the model [4] described in the introduction fits particularly well.

In [6] the Gilbert tessellation model is considered on  $\mathbb{R}^2$ , and it is assumed that the directions  $d_u$  are independent and uniformly distributed on  $[0, 2\pi]$ . Specifically, the rectangular case of Gilbert tessellation was first investigated in [7] where Gilbert's mean-field approach to study the distribution of the length of rays was further developed.

The approximation results of [7] for the rectangular Gilbert tessellation were further improved in [2] and [3]; moreover the latter works introduced a modification, the so-called "Half Gilbert tessellation" model for which a new technique was developed to get exact results on the distribution of the length of rays. It is argued in [3] that the results of the modified model give a good approximation for the original model. Still no exact results are available on the expected value of the line segments in the original Gilbert tessellation.

We take a different approach to study the original model. Namely, we derive bounds for the tail of the line distribution. Obviously, this does not yield the exact expectation, but the result allows to study the correlations in the model. It can be noted that the

derived here exponential bounds for the tail seem to be in line with the related limit theorems and the exponential fast stabilisation of the Gilbert tessellation proved in [8].

Very recently a new generalisation of Gilbert tessellation, namely "Iterated Gilbert mosaics", was introduced in [1]. The latter work opens a new perspective of Gilbert tessellation from a point of view of tropical geometry.

Our results on the quadrangulation process are stated in Section 2. The proofs are provided in Section 3.

## 2 Results

From now on we concentrate on the model given by Definition 1.2 with  $p = \frac{1}{2}$ , which we call **rectangular Gilbert tessellation model**.

### 2.1 Rectangular Gilbert tessellation model

At any time  $t \geq 0$  the state of the quadrangulation process according to Definition 1.2 is a set of rays, denote it  $G_N(t)$ . The initial state at  $t = 0$  is a random set of points  $\mathcal{V}_N$  in a box  $\Lambda_N$  generated by a Poisson process with intensity  $\lambda$ ; see (2). Each point  $v \in \mathcal{V}_N$  is equipped with random independent direction  $d_v$ , horizontal or vertical, equally probable ( $p = \frac{1}{2}$  in Definition 1.2).

For each direction, vertical or horizontal, we define as well the "+"-direction being "up" for vertical or "right" for horizontal, and the "-"-direction being "down" or "left", correspondingly. By Definition 1.2 from any  $v \in \mathcal{V}_N$  two rays start to grow at time  $t = 0$ ; correspondingly, denote them  $\mathcal{L}_v^\pm(t)$  with the obvious meaning that if the direction  $d_v$  is, for example, horizontal, then  $\mathcal{L}_v^+(t)$  is a ray to the right, and so on. Hence, writing  $\mathcal{L}_v^\pm(0) = v$ , we have for all  $t \geq 0$

$$G_N(t) := \{ \mathcal{L}_v^+(t), \mathcal{L}_v^-(t), v \in \mathcal{V}_N \}.$$

We shall also denote  $\mathcal{L}_v(t) = \mathcal{L}_v^+(t) \cup \mathcal{L}_v^-(t)$  the entire line that has grown from vertex  $v$  in both directions up to time  $t$ , and, correspondingly, we can write

$$G_N(t) := (\mathcal{L}_v(t), v \in \mathcal{V}_N).$$

As there are no more growing rays after time  $N$ , the set

$$G_N := G_N(N) = \{ \mathcal{L}_v^+ = \mathcal{L}_v^+(N), \mathcal{L}_v^- = \mathcal{L}_v^-(N), v \in \mathcal{V}_N \}.$$

is the final configuration which is indeed a random quadrangulation of  $\Lambda_N$ .

## 2.2 Tail for the lines distribution

The main question of interest is the distribution of the final length of a ray

$$L_v^\pm := |\mathcal{L}_v^\pm|.$$

Our aim is to study the probability of event

$$\{L_v = L_v^+ + L_v^- > x\}, \quad x > 0.$$

Note that if at time  $t$  a ray still grows, then its length at time  $t$  is

$$L_v^\pm(t) := |\mathcal{L}_v^\pm(t)| = t. \tag{3}$$

For example, for any given finite initial set  $\mathcal{V}_N$  there are small values  $t$  when each ray has equal length  $L_v^\pm(t) = t$  (see Figure 1). Hence, by (3)

$$\{L_v^\pm \geq t\} = \{L_v^\pm(t) = t\},$$

which shows that the distance and time could be interchangeable in this model due to a constant speed of growth. Therefore, we also mostly use the variable  $t$  for the distance.

It should be noted that each final  $L_v^\pm$  is also a function of  $N$ , since

$$L_v = L_v^+ + L_v^- \leq N.$$

However, notice that the bounds for the distribution tail stated below are uniform in  $N$ , and hold for the model on  $\mathbb{R}^2$ , i.e. when  $N \rightarrow \infty$ .

**Theorem 2.1.** *For any fixed  $\lambda > 0$  there are absolute positive constants  $c_1, c_2$  and  $\alpha_1 \geq \alpha_2$  such that*

$$c_1 e^{-\alpha_1 \sqrt{\lambda} t} \leq \mathbb{P}(L_v > t) \leq c_2 e^{-\alpha_2 \sqrt{\lambda} t}$$

for all  $t < \frac{N}{2}$ ,  $v \in \mathcal{V}_N$  and  $N$ .

Whether the distribution of the line segments is indeed exponential is not resolved by this result, although it shows a correct scaling for the expectation which is  $1/\sqrt{\lambda}$ . The latter simply reflects the following scaling property of the model. To underline the dependence on  $\lambda$  and  $N$ , let us write  $L_v = L_{v,\lambda,N}$ . Then it follows directly by the properties of the Poisson process that

$$L_{v,\lambda,N} \stackrel{d}{=} \frac{1}{\sqrt{\lambda}} L_{v,1,\sqrt{\lambda}N}.$$

One exact result on the model in a finite box  $\Lambda_N$  is the following curious fact about the number of rectangles.

**Proposition 2.1.** *The number of rectangles in the final quadrangulation of a finite box  $\Lambda_N$  equals*

$$|\mathcal{V}_N| + 1.$$

*Proof.* Follows by Euler's formula binding the number of vertices ( $V$ ), edges ( $E$ ) and faces ( $F$ ) for planar graphs:  $V + E + F = 2$ .  $\square$

## 2.3 Correlations

The core of difficulties in the analysis of Gilbert tessellation is in the strong spatial dependence. Therefore we begin to investigate the covariance structure of the model, which has not been done previously.

First we characterise some independent events in the model with help of the following construction.

**Definition 2.1.** *For each  $v \in \mathcal{V}_N$  and each ray  $\mathcal{L}_v^\pm(t)$  denote  $D_v^\pm(t)$  a square with a corner in  $v$ , whose diagonal from this corner has length  $2t$  along the ray  $\mathcal{L}_v^\pm(t)$ . Let  $C_v^\pm(t)$  denote the first half of this square, which is the cone with its top vertex at  $v$  and with  $\mathcal{L}_v^\pm(t)$  being its centre line; see Figure 3.*

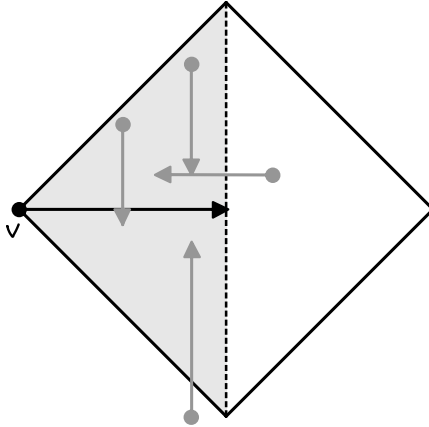


Figure 3: The shaded area is the cone  $C_v^+$ , the entire rotated square is the area of dependence  $D_v^+$ , including examples of other lines growing and influencing  $L_v^+$ .

We call  $D_v^\pm(t)$  the area of dependence for the event

$$A_v^\pm(t) := \{L_v^\pm(t) = t\}.$$

By the definition of our process a ray which might stop the growth of ray  $\mathcal{L}_v^\pm(s)$  before time  $t$ , can have its origin in the area  $C_v^\pm(t)$  only, while each of such rays in turn can be stopped within time  $t$  by another ray if the latter is originated in the area  $D_v^\pm(t)$  only. This observation leads to the following useful statement on independence checked by the same straightforward argument.

**Proposition 2.2.** *For any  $u, v \in \mathcal{V}_N$  and  $s, t > 0$  the events  $A_u^\pm(s)$  and  $A_v^\pm(t)$  are independent if and only if the corresponding areas of dependence do not intersect, i.e.*

$$D_u^\pm(s) \cap D_v^\pm(t) = \emptyset. \quad (4)$$

□

This proposition immediately yields independence of the rays growing from one point into different directions.

**Corollary 2.1.** *For any  $v \in \mathcal{V}_N$  the variables  $L_v^+(t)$  and  $L_v^-(s)$  are independent for all  $s, t$  such that  $s + t \leq N$ .*

□

Let us use here the following definition of distance.

**Definition 2.2.** *For any  $u, v \in \Lambda_N$  set*

$$\|u - v\|_1 = |u_1 - v_1| + |u_2 - v_2|.$$

Then for two different vertices  $u, v$  the areas of dependence  $D_u^\pm(t)$  and  $D_v^\pm(t)$  do not intersect at least up to time  $t = \|u - v\|_1/4$ . Note that the latter minimal time  $\|u - v\|_1/4$  until  $D_u^\pm(t)$  and  $D_v^\pm(t)$  meet (intersect) is achieved if  $|u_i - v_i| = 0$  for  $i$  along the direction of the rays when  $d_u = d_v$  or, in case of  $d_u \neq d_v$ , when  $3|u_i - v_i| = |u_j - v_j|, i \neq j \in \{1, 2\}$ . Hence, Proposition 2.2 implies in this case the following.

**Corollary 2.2.** *For any pair  $u, v \in \mathcal{V}_N$  the events  $\{L_u > t\}$  and  $\{L_v > t\}$  are independent for all  $t \leq \frac{1}{4}\|u - v\|_1$ .*

□

Generally speaking, the correlations and even their signs are involved and depend on the distances between the origins of the rays, the overlap of the areas of dependence and of course the directions of the rays.

In some cases the correlation sign is straightforward to establish. In particular, it is easy to construct an example where

$$\mathbb{P}\{(L_v^+ > t) \cap (L_u^+ > t)\} = 0. \quad (5)$$

Indeed, choose  $v = (v_1, v_2)$  and  $u = (u_1, u_2)$  with  $v_1 < u_1$  and  $v_2 > u_2$ . Then for any  $t > \|u - v\|_1$  we have (5), and hence,

$$\mathbb{P}\{(L_v^+ > t) \cap (L_u^+ > t)\} - \mathbb{P}\{L_v^+ > t\}\mathbb{P}\{L_u^+ > t\} < 0.$$

Consider a more complicated scenario. If two points in  $\mathcal{V}_N$  are close enough, then the lines growing from these points in the same direction are positively correlated, as stated below.

**Proposition 2.3.** *Let  $v, u \in \mathcal{V}_N$  be an arbitrary pair of points with equal orientation  $d_u = d_v$ . Suppose, that in the "+"-direction the distance between each vertex and the boundary of the box is at least  $\frac{N}{2}$ .*

*There is an absolute constant  $c_3$  such that if*

$$\|u - v\|_1 < c_3 \frac{e^{-\alpha_1 \sqrt{\lambda t}}}{\lambda t}$$

*( $\alpha_1$  is from Theorem 2.1), then*

$$\mathbb{P}\{(L_v^+ > t) \cap (L_u^+ > t)\} - \mathbb{P}\{L_v^+ > t\}\mathbb{P}\{L_u^+ > t\} > 0$$

*for all large  $N$  and large  $t < N$ . (A similar statement holds when the "+"-direction is replaced by the "-"-direction.)*

Finally, developing the results on independence and the exponential bounds for the tail for the distribution, we derive as well the exponential bound for decay of correlations of events  $\{L_u^\pm > t\}$  and  $\{L_v^\pm > t\}$  with respect to the distance between  $u$  and  $v$ .

**Theorem 2.2.** *Let  $v, u \in \mathcal{V}_N$  be an arbitrary pair of vertices. There are absolute positive constants  $c$  and  $\alpha$  such that*

$$|\mathbb{P}\{(L_v > t) \cap (L_u > t)\} - \mathbb{P}\{L_v > t\}\mathbb{P}\{L_u > t\}| \leq ce^{-\alpha\sqrt{\lambda}\|u-v\|_1}$$

*for all  $t$  and  $N$ .*

## 2.4 Percolation

Observe that the final quadrangulation of  $\Lambda_N$  does not change even if the growth of lines continues beyond the boundary of the box  $\Lambda_N$ . Assume here that the boundary of  $\Lambda_N$  does not stop the growth of rays. Nothing will prevent the growth outside of  $\Lambda_N$ , so all the rays which reach the boundary will grow unbounded towards infinity, correspondingly in four possible directions.

A phenomenon of reaching such state, called stabilisation, was studied in [8] for a more general model on  $\mathbb{R}^2$  with a finite number of the initial seeds and arbitrary directions.

**Definition 2.3** (Escaping rays). *Consider a realisation of the final quadrangulation. Call the rays that reach the border of  $\Lambda_N$  escaping rays.*

Thus the total number of escaping rays quantifies expansion of the model through a boundary. Recall that the number of initial seeds is a random  $\text{Poi}(\lambda N^2)$  variable. Hence, on the average the number of escaping rays could be of order  $N^2$ . However, as one may guess, the number is much less as we establish next.

**Theorem 2.3.** *Let  $\mathcal{R}_N$  be the number of escaping rays. For any  $\lambda > 0$  there are absolute constants  $C_1, C_2$  such that*

$$C_1\sqrt{\lambda}N \leq \mathbb{E}(\mathcal{R}_N) < C_2\sqrt{\lambda}N$$

for all large  $N$ .

## 3 Proofs

### 3.1 Proof of Theorem 2.1

Let  $v \in \mathcal{V}_N$  with a given orientation  $d_v$ . Without loss of generality we may assume that in "+" - direction the distance between  $v$  and the edge of the box  $\Lambda_N$  is at least  $\frac{N}{2}$ , and that the distance from  $v$  to the border of  $\Lambda_N$  in any direction is at least  $\frac{1}{\sqrt{\lambda}}$ . (Other cases are treated in a similar way with some obvious reduction.)

In a view of Corollary 2.1 we can study without loss of generality event  $\{L_v^+ > t\}$  for  $t > \frac{3}{\sqrt{\lambda}}$ . Consider Figure 3, where the half-diagonal of  $D_v^+$  is assumed to be equal to  $t$ . The event  $\{L_v^+ > t\}$  requires that all lines from points in  $C_v^+$  which grow orthogonal to  $\mathcal{L}_v^+$  are blocked by the lines parallel to  $\mathcal{L}_v^+$ . Hence, all points outside of such blocked areas should have orientation parallel to  $\mathcal{L}_v^+$ . This is depicted in Figure 4, where the points are crossed out in red if the (orthogonal to  $\mathcal{L}_v^+$ ) lines from them will be blocked by the lines from the blue points, those have to carry orientation parallel to  $\mathcal{L}_v^+$ . The latter are depicted together with a line-segment parallel to  $\mathcal{L}_v^+$ . The dashed lines mark the borders of the blocked areas. This picture instructs us to define the following notion of *tops*.

**Definition 3.1** (Tops). *For an arbitrarily fixed  $v \in \mathcal{V}_N$  with a given direction  $d_v$ , a point  $u \in C_v(t)$  is called a top with respect to  $\mathcal{L}_v^+$ , if*

$$\{L_v^+ \geq t\} \cap \{d_u \neq d_v\} = \emptyset.$$

In other words, a point  $u \in C_v$  is called a top if, in order to possibly yield  $\{L_v^+ \geq t\}$ ,  $d_u$  must be of the same orientation as  $d_v$ . Observe, that the definition of a top is relative: whether  $u$  is a "top" depends on  $\mathcal{L}_v^+$  and set  $\mathcal{V}_N$ .

To find bounds for  $\mathbb{P}\{L_v^+ > t\}$  we shall first consider the impact of points of  $\mathcal{V}_N$  close to  $\mathcal{L}_v^+$ . Let us divide  $C_v^+$  into the following subareas. Define an area of width  $\frac{1}{\sqrt{\lambda}}$  that is adjacent to  $\mathcal{L}_v^+$  on an arbitrarily fixed side, and is of length  $t$  (see area shaded red in Figure 5). We shall refer to it as *stripe* and denote it by  $S_v$ .

We observe that, for  $L_v^+ \geq t$  to hold, it is a necessary condition that the lines from all points in  $S_v$  do not cross  $\mathcal{L}_v^+$ . This is necessary for the stripes on both sides. Call  $S'_v$  the

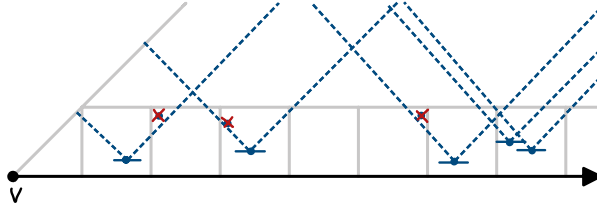


Figure 4: Illustration of *tops*. The horizontal arrow of length  $t$  represents  $\mathcal{L}_v^+(t)$ . Blue points with small lines are the tops. Points that are crossed out in red are not tops, because they are blocked by lines of other points. The narrow stripe  $S_v$  is divided into small boxes.

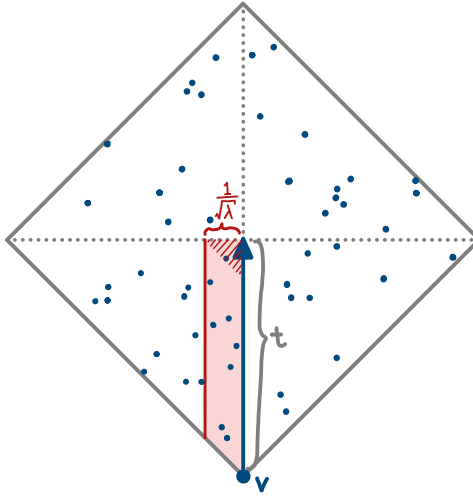


Figure 5: Illustration of the stripe  $S_v$  of width  $\frac{1}{\sqrt{\lambda}}$  and length  $t$ , shaded in red.

equal stripe on the other side. Let us define the following events:

$$\begin{aligned}
 B &:= \{\text{no lines from points in stripe } S_v \text{ cross } \mathcal{L}_v^+\}, \\
 B' &:= \{\text{no lines from points in stripe } S'_v \text{ cross } \mathcal{L}_v^+\}, \\
 \bar{B} &:= \{\text{no lines from points in } C_v \setminus (S_v \cup S'_v) \text{ cross } \mathcal{L}_v^+\}.
 \end{aligned}$$

Then,

$$B \cap B' \cap \bar{B} = \{L_v^+ > t\} \tag{6}$$

and thus

$$\{L_v^+ > t\} \subseteq B \cap B',$$

which implies

$$\mathbb{P}(L_v^+ > t) \leq \mathbb{P}(B \cap B').$$

Note that the events  $B$  and  $B'$  are not independent: indeed, the lines from points in a triangle in the square in the stripe  $S_v$  furthest away from  $v$  (the striped area in Figure 5) can indirectly influence what happens in the corresponding area in the other stripe  $S'_v$ .

Let us modify the stripes so that there is no above mentioned interference, simply by cutting away certain parts. Let  $\tilde{S}_v$  be the rectangle within  $S_v$  of a size

$$\frac{1}{\sqrt{\lambda}} \times \frac{\lceil t\sqrt{\lambda} \rceil - 2}{\sqrt{\lambda}} \quad (7)$$

along the interval  $[0, t]$ .

Similarly, we define a stripe  $\tilde{S}'_v \subset S'_v$  on the other side of  $\mathcal{L}_v^+$ . We also define the corresponding events:

$$\begin{aligned} \tilde{B} &:= \{\text{no lines from points in the adjusted stripe } \tilde{S}_v \text{ cut off } L_v^+\} \supseteq B, \\ \tilde{B}' &:= \{\text{no lines from points in the adjusted stripe } \tilde{S}'_v \text{ cut off } L_v^+\} \supseteq B', \end{aligned} \quad (8)$$

which are independent and have the same probability due to symmetry. Hence,

$$\mathbb{P}(L_v^+ > t) \leq \mathbb{P}(B \cap B') \leq \mathbb{P}(\tilde{B} \cap \tilde{B}') = \left(\mathbb{P}(\tilde{B})\right)^2. \quad (9)$$

Consider event  $\tilde{B}$  with the help of the notion "top" introduced above. First, taking into account (7) we shall divide the stripe  $\tilde{S}_v$  into

$$n_t = \lceil t\sqrt{\lambda} \rceil - 2 \geq t\sqrt{\lambda} - 3 \quad (10)$$

squares (or boxes) with side length  $\frac{1}{\sqrt{\lambda}}$  as illustrated in Figure 4.

Let  $W$  denote the (random) number of boxes in  $\tilde{S}_v$  that contain at least one point of  $\mathcal{V}_N$ , i.e. that are non-empty. Then there are at least  $\max\{0, (\lfloor \frac{W}{3} \rfloor - 2)\}$  tops in area  $\tilde{S}_v$  because of the following arguments. Note that the line grown in the direction orthogonal to  $\mathcal{L}_v$  from any vertex in any box in  $\tilde{S}_v$  can be blocked (i.e. prevented crossing  $\mathcal{L}_v^+$ ) by a line from another vertex if only either the latter vertex belongs to the same box, or to one of the two neighbouring boxes. Hence,

$$M := \#\{\text{tops in } \tilde{S}_v\} \geq \left\lfloor \frac{W}{3} \right\rfloor - 2. \quad (11)$$

Consider now

$$\mathbb{P}(\tilde{B}) = \mathbb{E}\mathbb{P}(\tilde{B}|M). \quad (12)$$

The event  $\tilde{B}$  (see (8)) requires that all tops are assigned orientation  $d_v$ , which has probability  $\frac{1}{2}$  for each top independently. This allows us to derive from (12)

$$\begin{aligned} \mathbb{P}(\tilde{B}) &\leq \sum_{m=0}^{\gamma} \mathbb{P}(M = m) + \sum_{m=\gamma+1}^{\infty} \mathbb{P}(\tilde{B}|M = m) \\ &= \mathbb{P}(M \leq \gamma) + \sum_{m=\gamma+1}^{\infty} \left(\frac{1}{2}\right)^m = \mathbb{P}(M \leq \gamma) + \left(\frac{1}{2}\right)^{\gamma} \end{aligned} \quad (13)$$

for an arbitrary  $\gamma$ , which should be chosen in some optimal way. By (11)

$$\mathbb{P}(M \leq \gamma) \leq \mathbb{P}(W \leq 3\gamma + 8),$$

where  $W$  is the number of non-empty boxes among  $n_t$  boxes. Recall that the area of each box is  $1/\lambda$ , and the points are distributed as Poisson process with intensity  $\lambda$ , implying that the numbers of points in different boxes are independent and distributed as  $\text{Poi}(1)$ . Hence, the probability that a box is non-empty is  $1 - e^{-1}$ , and the total number of non-empty boxes has Binomial distribution:

$$W \sim \text{Bin}(n_t, 1 - e^{-1}). \quad (14)$$

By the Chernoff bound for all  $0 < \vartheta < 1$

$$\mathbb{P}\{W \leq \mathbb{E}W(1 - \vartheta)\} \leq \exp\left\{-\frac{\vartheta^2}{2}\mathbb{E}W\right\}.$$

Choosing now  $\gamma$  in (13) so that

$$3\gamma + 8 = \lceil \mathbb{E}W(1 - \vartheta) \rceil$$

for  $0 < \vartheta < 1$  to be chosen later, we derive from (13)

$$\mathbb{P}(\tilde{B}) \leq \exp\left(-\frac{1}{2}\vartheta^2\mathbb{E}W\right) + \exp\left(-\frac{\ln(2)}{3}(1 - \vartheta)\mathbb{E}W + 3\ln(2)\right), \quad (15)$$

where

$$\mathbb{E}W = n_t(1 - e^{-1}) = (\lfloor t\sqrt{\lambda} \rfloor - 2)(1 - e^{-1}) \geq (t\sqrt{\lambda} - 3)(1 - e^{-1}).$$

As we are interested in the large values for  $t$ , the optimal value for  $\vartheta$  matching the exponents in (15) must satisfy

$$\frac{1}{2}\vartheta^2 = \frac{\ln(2)}{3}(1 - \vartheta),$$

which is

$$\vartheta = -\frac{\ln(2)}{3} + \sqrt{\frac{\ln(2)^2}{9} + \frac{2\ln(2)}{3}}.$$

With the last choice of  $\vartheta$  the bound in (15) reads as

$$\begin{aligned} \mathbb{P}(\tilde{B}) &\leq \left( \exp\left(\frac{3}{2}(1-e^{-1})\vartheta^2\right) + \left(\frac{1}{2}\right)^{-(3+(1-\vartheta)(1-\frac{1}{e}))} \right) \exp\left(-\frac{\vartheta^2}{2}(1-e^{-1})\sqrt{\lambda t}\right) \\ &=: ce^{-\alpha\sqrt{\lambda t}}, \end{aligned}$$

where  $c$  and  $\alpha$  are absolute positive constants. Substituting the last bound into (9) we get

$$\mathbb{P}(L_v^+ > t) \leq c^2 e^{-2\alpha\sqrt{\lambda t}}.$$

By the symmetry the same bound holds for the tail of  $L_v^-$  as well, hence,

$$\mathbb{P}(L_v > t) \leq c_2 e^{-\alpha_2\sqrt{\lambda t}} \quad (16)$$

for some absolute positive constants  $c_2$  and  $\alpha_2$ , which is the upper bound in the statement of the theorem.

Let us now turn to the lower bound.

Recall the relation (6). This time we rewrite it with the help of the events

$$B_1 := \{\mathcal{L}_v^+ \text{ is not crossed by lines from points in } C_v \text{ on the side of } S_v\}, \quad (17)$$

$$B'_1 := \{\mathcal{L}_v^+ \text{ is not crossed by lines from points in } C_v \text{ on the opposite to } S_v \text{ side}\},$$

so that

$$B_1 \cap B'_1 = \{L_v^+ > t\}. \quad (18)$$

We shall find events which yield, correspondingly, each of the events on the left side of (18). First we consider again a stripe  $S_v$  of width  $1/\sqrt{\lambda}$  along  $\mathcal{L}_v^+$ ; see Figure 6. Suppose a configuration  $\mathcal{V}_N$  has some vertices in  $S_v$ . Then the lines from the points which are tops in  $S_v$  with assigned orientation  $d_v$  will block the lines from vertices in their respective dependence areas (these are shaded areas above the tops, we call it *blocked area*), and thus yield event  $B_1$  if no other lines outside of the blocked areas cross  $\mathcal{L}_v^+$ .

To formalise this construction, we shall use again set  $\tilde{S}_v \subset S_v$  divided into  $n_t$  equal boxes. This is the set where we consider the locations of tops induced by the configuration  $\mathcal{V}_N$ . Let  $X$  denote the number of empty boxes among  $n_t$  boxes (see (10)), and then denote  $S_v^X$  the subset of  $C_v^+$  which is not blocked by the tops in  $\tilde{S}_v$ . Then as argued above, for a given configuration  $\mathcal{V}_N$  with a fixed  $X = x$  the event

$$B_x := \{\text{all points in } S_v^x \text{ have the same orientation as } v\}$$

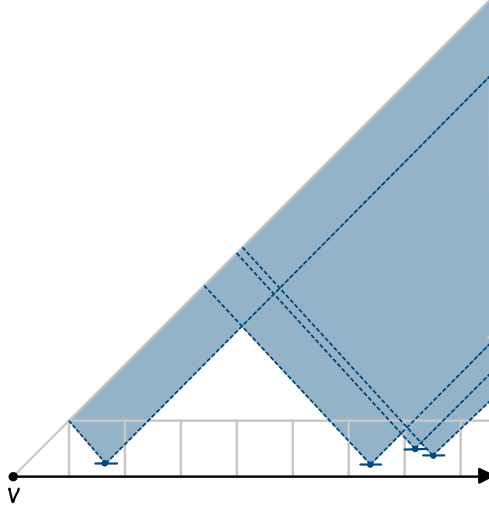


Figure 6: Illustration of the area where the orientation of points does not affect  $\{L_v > t\}$ , shaded in blue. I.e., the area blocked by lines from tops. The line  $\mathcal{L}_v^+$  is of length  $t$ .

yields event  $B_1$  defined in (17), i.e.

$$B_x \subseteq B_1.$$

We shall also define event  $B_X$  such that  $\mathbb{P}\{B_X | X = x\} = \mathbb{P}\{B_x\}$ .

Similar construction of a set  $B'_{X'}$ , on the other side of  $\mathcal{L}^+$ , where  $X'$  is an independent copy of  $X$ , gives us

$$B'_{x'} \subseteq B'_1,$$

and hence, for any realisation  $X = x, X' = x'$

$$B_x \cap B'_{x'} \subseteq B_1 \cap B'_1,$$

which yields

$$\mathbb{P}\{B_X \cap B'_{X'}\} \leq \mathbb{P}\{B_1 \cap B'_1\}. \quad (19)$$

As the events on the left are conditionally independent due to construction and the properties of a Poisson process, we have

$$\mathbb{E}\mathbb{P}\{B_X \cap B'_{X'} | X, X'\} = \mathbb{E}\mathbb{P}\{B_X | X\} \mathbb{E}\mathbb{P}\{B'_{X'} | X'\} = (\mathbb{P}\{B_X\})^2, \quad (20)$$

where the last equality is by symmetry. Our aim now is for any admissible value  $X = x$  to bound from below the probability  $\mathbb{P}(B_x) = \mathbb{P}(B_X | X = x)$ .

The number of vertices from  $\mathcal{V}_N$  which belong to  $S_v^x$  with an area  $A(S_v^x)$  follows  $\text{Poi}(A(S_v^x)\lambda)$  distribution. Hence, setting  $Y \sim \text{Poi}(A(S_v^x)\lambda)$  we get

$$\mathbb{P}(B_x) = \mathbb{E} \left( \frac{1}{2} \right)^Y, \quad (21)$$

which is a decreasing function of the area  $A(S_v^x)$  by the properties of Poisson process. Therefore for a given number  $x$  we shall identify the case of smallest possible blocked area, so that the complement to it, which has area  $A(S_v^x)$ , is the largest among configurations  $\mathcal{V}_N$  which leave exactly  $x$  empty boxes in  $\tilde{S}_v$ ; see some examples in Figure 7.

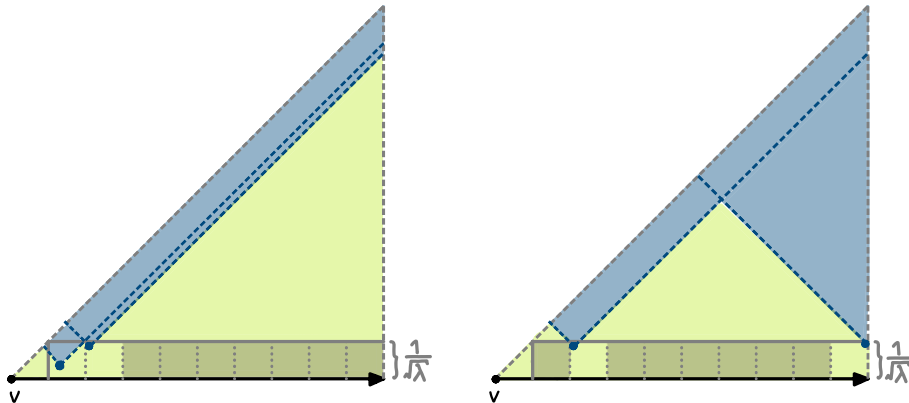


Figure 7:  $S_v^x$  shaded in light green, with the example of  $x = 7$  empty boxes (shaded darker) in different positions.

Clearly,  $A(S_v^x)$  depends on  $x$ . For example, when all  $n_t$  boxes are empty the set  $S_v^x$  is simply the entire  $C_v^+ \setminus \tilde{S}_v$ , area of which is at most  $t^2/2$ . Inspecting Figure 7 it is straightforward to derive the following bound for all  $x$ :

$$A(S_v^x) \leq \frac{1}{2\lambda}(x+2)^2 + (n_t - x)\frac{1}{2\lambda} + \frac{1}{2\lambda} =: A_x, \quad (22)$$

where the last term in the middle sum corresponds the end part of  $\tilde{S}_v$ . Bound (22) is uniform for all configurations  $\mathcal{V}_N$  which leave exactly  $x$  empty boxes in  $\tilde{S}_v$ . Denoting

$$Y_x \sim \text{Poi}(A_x \lambda)$$

we derive from (21)

$$\mathbb{P}(B_x) \geq \mathbb{E} \left( \frac{1}{2} \right)^{Y_x} = e^{-\frac{A_x \lambda}{2}}. \quad (23)$$

Recall that  $X$  is the number of empty boxes, and thus (similar to (14))

$$X \stackrel{d}{=} \sum_{i=1}^{n_t} \xi_i, \quad (24)$$

where  $\xi_i$  are independent  $Be(\frac{1}{e})$  random variables. Therefore by (23) and (24) we get the following bound

$$\mathbb{P}(B_X) \geq \mathbb{E} e^{-\frac{A_X \lambda}{2}} = e^{-\frac{1}{4}(5+n_t)} \mathbb{E} e^{-\frac{1}{4}(X^2+3X)} \geq e^{-\frac{1}{4}(5+n_t)} \left( \mathbb{E} e^{-\frac{1}{4}(2\xi_1^2+3\xi_1)} \right)^{n_t}$$

$$= e^{-\frac{5}{4}} \left( e^{-\frac{1}{4}} \mathbb{E} e^{-\frac{1}{4}(2\xi_1^2 + 3\xi_1)} \right)^{n_t}.$$

Taking into account (10) we derive from here

$$\mathbb{P}(B_X) \geq c_1 e^{-\alpha_1 \sqrt{\lambda} t}$$

for the absolute constants

$$c_1 = e^{-\frac{5}{4}}, \quad \alpha_1 = \frac{1}{4} - \ln \left( (1 - e^{-1}) + e^{-1} e^{-\frac{5}{4}} \right).$$

Substituting the last bound into (20) and making use of the result in (19) we get

$$\mathbb{P}\{B_1 \cap B'_1\} \geq c_1^2 e^{-2\alpha_1 \sqrt{\lambda} t}.$$

Finally, by the relation (18) this yields the lower bound

$$\mathbb{P}\{L_v^+ > t\} \geq c_1^2 e^{-2\alpha_1 \sqrt{\lambda} t}.$$

By symmetry the same bound holds when  $L_v^+$  is replaced by  $L_v^-$ . Therefore

$$\mathbb{P}\{L_v > t\} \geq \max\{\mathbb{P}\{L_v^+ > t\}, \mathbb{P}\{L_v^- > t\}\} \geq c_1^2 e^{-2\alpha_1 \sqrt{\lambda} t}.$$

This together with the upper bound (16) completes the proof of Theorem 2.1.  $\square$

### 3.2 Proof of Proposition 2.3

For given  $u, v$  with  $\|u - v\|_1 = d$ , and  $t$  consider the areas of dependence  $D_v^+(t)$  and  $D_u^+(t)$ . Let  $\mathcal{C}$  denote the central area between the rays  $\mathcal{L}_v^+$  and  $\mathcal{L}_u^+$  within the union  $D_v^+(t) \cup D_u^+(t)$  (see Figure 8), and then define another set

$$\mathcal{B} = \mathcal{C} \cup (D_v^+(t) \Delta D_u^+(t)) \cup (C_v^+(t) \Delta C_u^+(t)).$$

This is illustrated in Figure 8, where  $\mathcal{B}$  is shaded in grey. Then we observe that

$$\{L_v^+ > t\} \cap \{\mathcal{B} \cap \mathcal{V}_N = \emptyset\} = \{L_u^+ > t\} \cap \{\mathcal{B} \cap \mathcal{V}_N = \emptyset\} \quad (25)$$

$$= \{L_v^+ > t\} \cap \{L_u^+ > t\} \cap \{\mathcal{B} \cap \mathcal{V}_N = \emptyset\} \subseteq \{L_v^+ > t\} \cap \{L_u^+ > t\},$$

where the number of points in  $\{\mathcal{B} \cap \mathcal{V}_N\}$  has a Poisson distribution. More precisely, if  $A(\mathcal{B})$  denotes the area of  $\mathcal{B}$ , then

$$|\{\mathcal{B} \cap \mathcal{V}_N\}| \sim \text{Poi}(A(\mathcal{B})\lambda).$$

Note that  $\mathcal{B}$  is the area along the square (perimeter of  $D_v$ ) and its two diagonals, which admits a bound

$$A(\mathcal{B}) < 4(1 + \sqrt{2})(t + d)d =: c(t + d)d.$$

Making use of this bound we get

$$\mathbb{P}\{\mathcal{B} \cap \mathcal{V}_N = \emptyset\} \geq e^{-\lambda c(t+d)d}. \quad (26)$$

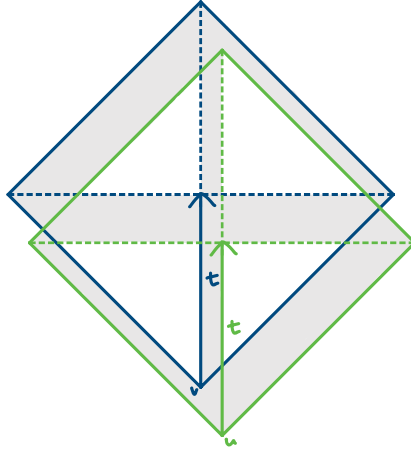


Figure 8: Illustration of the constructed area  $\mathcal{B}$ , shaded in grey.

Therefore by (25) and (26)

$$\begin{aligned} \mathbb{P}\{(L_v^+ > t) \cap (L_u^+ > t)\} &\geq \mathbb{P}\{\{L_v^+ > t\} \cap \{\mathcal{B} \cap \mathcal{V}_N = \emptyset\}\} \\ &= \mathbb{P}\{L_v^+ > t\} - \mathbb{P}\{\{L_v^+ > t\} \cap \{\mathcal{B} \cap \mathcal{V}_N \neq \emptyset\}\} \\ &\geq \mathbb{P}\{L_v^+ > t\} - \mathbb{P}\{\mathcal{B} \cap \mathcal{V}_N \neq \emptyset\} \geq \mathbb{P}\{L_v^+ > t\} - (1 - e^{-c\lambda(t+d)d}). \\ &\geq \mathbb{P}\{L_v^+ > t\} - \lambda c(t + d)d. \end{aligned}$$

With this bound we derive

$$\begin{aligned} &\mathbb{P}\{(L_v^+ > t) \cap (L_u^+ > t)\} - \mathbb{P}\{L_v^+ > t\}\mathbb{P}\{L_u^+ > t\} \\ &\geq \mathbb{P}\{L_v^+ > t\} (1 - \mathbb{P}\{L_u^+ > t\}) - c\lambda(t + d)d. \end{aligned}$$

Substituting in the last formula the upper and the lower bounds established in Theorem 2.1 we obtain

$$\begin{aligned} &\mathbb{P}\{(L_v^+ > t) \cap (L_u^+ > t)\} - \mathbb{P}\{L_v^+ > t\}\mathbb{P}\{L_u^+ > t\} \\ &\geq c_1 e^{-\alpha_1 \sqrt{\lambda} t} (1 - c_2 e^{-\alpha_2 \sqrt{\lambda} t}) - c\lambda(t + d)d, \end{aligned}$$

which is positive if

$$d < c_3 \frac{e^{-\alpha_1 \sqrt{\lambda} t}}{\lambda t},$$

where  $c_3 > 0$  is an absolute constant. □

### 3.3 Proof of Theorem 2.2

Assume,  $t > \frac{1}{4} \|u - v\|_1$ . Otherwise, the statement is trivial due to Corollary 2.2.

Note that for any  $t' < t$

$$\mathbb{P}\{(L_v > t) \cap (L_u > t)\} \leq \mathbb{P}\{(L_v > t') \cap (L_u > t')\}.$$

Setting now

$$t' = \frac{1}{4} \|u - v\|_1,$$

and applying Corollary 2.2 we get

$$\begin{aligned} \mathbb{P}\{(L_v > t) \cap (L_u > t)\} &\leq \mathbb{P}\left\{\left(L_v > \frac{1}{4} \|u - v\|_1\right) \cap \left(L_u > \frac{1}{4} \|u - v\|_1\right)\right\} \\ &= \mathbb{P}\left\{L_v > \frac{1}{4} \|u - v\|_1\right\} \mathbb{P}\left\{L_u > \frac{1}{4} \|u - v\|_1\right\}. \end{aligned}$$

Hence,

$$|\mathbb{P}\{(L_v > t) \cap (L_u > t)\} - \mathbb{P}\{L_v > t\} \mathbb{P}\{L_u > t\}| \leq 2 \left( \mathbb{P}\left\{L_v > \frac{1}{4} \|u - v\|_1\right\} \right)^2.$$

Finally, applying Theorem 2.1 we derive

$$|\mathbb{P}\{(L_v > t) \cap (L_u > t)\} - \mathbb{P}\{L_v > t\} \mathbb{P}\{L_u > t\}| \leq 2c_2^2 e^{-\alpha_2 \sqrt{\lambda} \frac{1}{2} \|u - v\|_1},$$

which yields the statement of the theorem. □

### 3.4 Proof of Theorem 2.3

For any  $v \in \mathcal{V}_N$  let us introduce the events

$$B_v^\pm := \{\mathcal{L}_v^\pm \text{ reaches the border of } \Lambda_N\}.$$

Our aim is to study the expectation of

$$\mathcal{R}_N := \sum_{v \in \mathcal{V}_N} (\mathbb{1}\{B_v^+\} + \mathbb{1}\{B_v^-\}).$$

Given a set  $\mathcal{V}_N$  let  $U$  denote a random point chosen uniformly in  $\mathcal{V}_N$ . Then we can write

$$\begin{aligned}\mathbb{E}\mathcal{R}_N &= \mathbb{E} \sum_{v \in \mathcal{V}_N} (\mathbb{1}\{B_v^+\} + \mathbb{1}\{B_v^-\}) \\ &= \mathbb{E} (|\mathcal{V}_N| \mathbb{E} \{ (\mathbb{1}\{B_U^+\} + \mathbb{1}\{B_U^-\}) | |\mathcal{V}_N| \}).\end{aligned}\tag{27}$$

Consider events  $B_U^\pm$ . Letting  $\eta_U^\pm$  denote the distance from  $U$  to the boundary of  $\Lambda_N$  in the direction of  $\mathcal{L}_U^\pm$  correspondingly, we have

$$B_U^\pm = \{L_U^\pm \geq \eta_U^\pm\},$$

and we rewrite (27) as

$$\mathbb{E}\mathcal{R}_N = \mathbb{E} (|\mathcal{V}_N| \mathbb{E} \{ \mathbb{1}\{L_U^+ \geq \eta_U^+\} | |\mathcal{V}_N| \}) + \mathbb{E} (|\mathcal{V}_N| \mathbb{E} \{ \mathbb{1}\{L_U^- \geq \eta_U^-\} | |\mathcal{V}_N| \}).\tag{28}$$

We shall make use of the property of Poisson process that conditionally on a positive number  $|\mathcal{V}_N|$  the distance  $\eta_U^+$  is uniformly distributed on the entire interval  $[0, N]$ . Denote  $T \sim U([0, N])$  a random variable uniformly distributed on  $[0, N]$  independent of  $|\mathcal{V}_N|$ . Then we can rewrite the terms in (28) as follows

$$\begin{aligned}&\mathbb{E} (|\mathcal{V}_N| \mathbb{E} \{ \mathbb{1}\{L_U^+ \geq \eta_U^+\} | |\mathcal{V}_N| \}) \\ &= \mathbb{E} (|\mathcal{V}_N| \mathbb{E} \{ \mathbb{1}\{L_U^+ \geq T\} | |\mathcal{V}_N| \}) \\ &= \mathbb{E} \{ \mathbb{E} (|\mathcal{V}_N| \mathbb{E} \{ \mathbb{1}\{L_U^+ \geq T\} | |\mathcal{V}_N| \}) | T \} \\ &= \int_0^N \frac{1}{N} \mathbb{E} (|\mathcal{V}_N| \mathbb{E} \{ \mathbb{1}\{L_U^+ \geq t\} | |\mathcal{V}_N| \}) dt.\end{aligned}\tag{29}$$

For any  $t > 0$  we derive with the help of Cauchy-Bounyakovskii inequality

$$\begin{aligned}&\mathbb{E} (|\mathcal{V}_N| \mathbb{E} \{ \mathbb{1}\{L_U^+ \geq t\} | |\mathcal{V}_N| \}) \\ &\leq (\mathbb{E}|\mathcal{V}_N|^2)^{1/2} \left( \mathbb{E} (\mathbb{E} \{ \mathbb{1}\{L_U^+ \geq t\} | |\mathcal{V}_N| \})^2 \right)^{1/2} \\ &\leq (\mathbb{E}|\mathcal{V}_N|^2)^{1/2} (\mathbb{E}\mathbb{E} \{ \mathbb{1}\{L_U^+ \geq t\} | |\mathcal{V}_N| \})^{1/2} \\ &= (\mathbb{E}|\mathcal{V}_N|^2)^{1/2} (\mathbb{P} \{L_U^+ \geq t\})^{1/2}.\end{aligned}$$

With the help of the uniform bound from Theorem 2.1 we obtain from here

$$\begin{aligned}&\mathbb{E} (|\mathcal{V}_N| \mathbb{E} \{ \mathbb{1}\{L_U^+ \geq t\} | |\mathcal{V}_N| \}) \\ &\leq (\mathbb{E}|\mathcal{V}_N|^2)^{1/2} \left( c_2 e^{-\alpha_2 \sqrt{\lambda} t} \right)^{1/2} = \left( \lambda N^2 + (\lambda N^2)^2 \right)^{1/2} \left( c_2 e^{-\alpha_2 \sqrt{\lambda} t} \right)^{1/2}\end{aligned}$$

$$\leq c_3 \lambda N^2 e^{-\alpha_3 \sqrt{\lambda} t}$$

for all large  $N$  and some absolute constants  $c_3, \alpha_3$ . Substituting the last bound into (29) we derive

$$\begin{aligned} & \mathbb{E} (|\mathcal{V}_N| \mathbb{E} \{ \mathbb{1}\{L_U^+ \geq \eta_U^+\} | |\mathcal{V}_N| \}) \\ &= \int_0^N \frac{1}{N} \mathbb{E} \{ (|\mathcal{V}_N| \mathbb{E} \{ \mathbb{1}\{L_U^+ \geq t\} | |\mathcal{V}_N| \}) \} dt \leq c_4 \sqrt{\lambda} N \end{aligned} \quad (30)$$

for some absolute constant  $c_4$ . By the symmetry the same bound holds for the last term in (28), yielding together with (30)

$$\mathbb{E} \mathcal{R}_N \leq 2c_4 \sqrt{\lambda} N,$$

which is the upper bound in Theorem 2.3.

Next, we derive the lower bound. For that we shall simply count the escaping rays that originated in a narrow band of width  $\frac{1}{\sqrt{\lambda}}$  at the boundary of box  $\Lambda_N$ , as illustrated in Figure 9. Cutting away the corner squares, also with side length  $\frac{1}{\sqrt{\lambda}}$ , leaves the four stripes  $S_1, \dots, S_4$ , shaded red in that figure. The numbers of escaping rays from each of the stripes are equally distributed due to the symmetry.

Recall the Definition 3.1 of the notion "top". This time we use it replacing the line  $\mathcal{L}_v^\pm$  by the segment of the border through which there is a possible escape. Then by this definition if a top vertex has orientation orthogonal to the closest border of  $\Lambda_N$ , it is guaranteed to have an escaping line from this vertex. This is illustrated in the example stripe  $S_2$  in the figure as well.

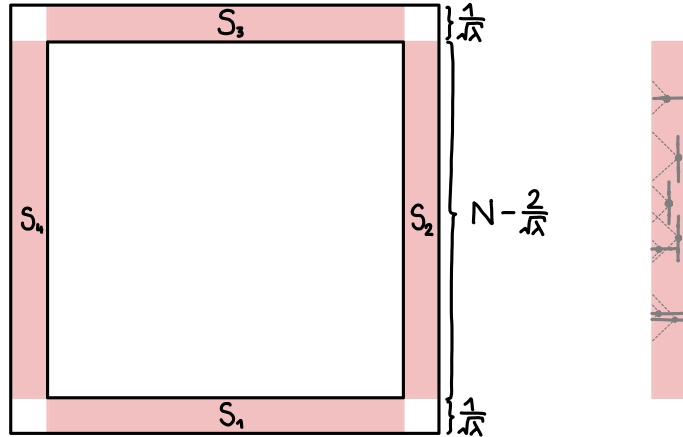


Figure 9: Illustration of the frame of width  $\frac{1}{\sqrt{\lambda}}$  and stripes  $S_1, \dots, S_4$ . On the right side, an example of  $S_2$  with tops and vertices that are not tops whose lines reach the border.

Hence, if  $M_1$  is the number of tops in one stripe (say,  $S_2$  in Figure 9) of length  $N - \frac{2}{\sqrt{\lambda}}$  and width  $\frac{1}{\sqrt{\lambda}}$ , then we have a rough lower bound in a form

$$\mathbb{E}\mathcal{R}_N \geq 4\mathbb{E}M_1/2, \quad (31)$$

where 4 represents 4 sides, and  $\frac{1}{2}$  is the probability that a vertex has the required orientation.

To find a lower bound for  $M_1$  let us divide the above stripe (of length  $N - \frac{2}{\sqrt{\lambda}}$  and width  $\frac{1}{\sqrt{\lambda}}$ ) into boxes with side length  $\frac{1}{\sqrt{\lambda}}$ . This gives us

$$n := \left\lfloor \sqrt{\lambda} \left( N - \frac{2}{\sqrt{\lambda}} \right) \right\rfloor \geq \sqrt{\lambda}N - 3$$

whole non-intersecting squares with side length  $\frac{1}{\sqrt{\lambda}}$ . Let  $M$  be the total number of tops in these  $n$  boxes, and let  $W$  be the number of non-empty boxes. Notice, that  $M \leq M_1$ . As the number of points in each box follows a Poi(1) distribution independently for all boxes, the distribution of  $W$  is Binomial:

$$W \sim \text{Bin} \left( n, 1 - \frac{1}{e} \right).$$

As we argued in the proof of Theorem 2.1 (see (11)), it holds that

$$M \geq \left\lfloor \frac{W}{3} \right\rfloor - 2.$$

Combining these facts we derive from (31)

$$\mathbb{E}\mathcal{R}_N \geq 2\mathbb{E}M \geq 2\mathbb{E} \left( \left\lfloor \frac{W}{3} \right\rfloor - 2 \right) \geq \frac{2}{3}\sqrt{\lambda} \left( 1 - \frac{1}{e} \right) N - 8,$$

which confirms the lower bound in the statement of the theorem.  $\square$

## Acknowledgements

This work was supported by a fellowship of the German Academic Exchange Service (DAAD) for the author Emily Ewers.

## References

- [1] Baccelli, F. and Tran, N. M. (2022) Iterated Gilbert mosaics. *Stochastic Process. Appl.* 150, 752–781.

- [2] Burridge, J. and Cowan, R. (2016) Planar tessellations that have the half-Gilbert structure. *Advances in Applied Probability*, 48 (2), 574–584. doi: 10.1017/apr.2016.15
- [3] Burridge, J., Cowan, R., and Ma, I. (2013) Full- and half-Gilbert tessellations with rectangular cells. *Advances in Applied Probability*, 45 (1), 1-19. doi: 10.1239/aap/1363354100
- [4] Ekström, H. and Turova, T. (2022) Non-monotone cellular automata: order prevails over chaos. *BioSystems*, 220. doi: 10.1016/j.biosystems.2022.104756
- [5] Gilbert, E. N. (1962) Random subdivisions of space into crystals. *Ann. Math. Statist.* 33, 958–972.
- [6] Gilbert, E. N. (1967) Random plane networks and needle-shaped crystals. In Noble, B. (ed.), *Applications of Undergraduate Mathematics in Engineering*, New York: Macmillan.
- [7] Mackisack, M. S. and Miles, R. E. (1996) Homogeneous rectangular tessellations. *Advances in Applied Probability*, 28 (4), 993–1013. doi: 10.2307/1428161.
- [8] Schreiber, T. and Soja, N. (2011) Limit theory for planar Gilbert tessellations. *Probab. Math. Statist.* 31 (1), 149–160.